IEEE Access
Multidisciplinary ⋮ Rapid Review ⋮ Open Access Journal

Received August 7, 2019, accepted August 12, 2019, date of publication August 20, 2019, date of current version September 4, 2019.

Digital Object Identifier 10.1109/ACCESS.2019.2936496

Effects of Wear, Backlash, and Bearing Clearance on Dynamic Characteristics of a Spur Gear System

YING-KUI GU, WEN-FEI LI, JUN ZHANG, AND GUANG-QI QIU
School of Mechanical and Electrical Engineering, Jiangxi University of Science and Technology, Ganzhou 341000, China

Corresponding author: Guang-Qi Qiu (guyingkui@163.com)

This research was partially supported by the National Natural Science Foundation of China under the contract number 61463021 and 61963018, the Natural Science Foundation of Jiangxi Province under the contract number 20181BAB202020, and the Young Scientists Object Program of Jiangxi Province, China under the contract number 20144BCB23037.

ABSTRACT A six-degree-of-freedom gear pair torsional vibration model considering time-varying stiffness, damping, dynamic backlash, bearing radial clearance and comprehensive wear of the tooth surface is established by using the lumped mass method in this paper. According to the comprehensive wear of tooth surface, the wear severity is divided into non-wear, slight wear and severe wear. The triangular function is used to simulate the wear failure of tooth surface. The effects of backlash, bearing clearance and comprehensive wear of tooth surface on the steady-state response of the gear system are analyzed respectively. The results show that the radial clearance of the bearing intensifies the vibration and causes the step phenomenon at high speed. The backlash increases the amplitude of vibration, the meshing force and the impact of back of teeth. Moreover, the side frequency bands generated by amplitude modulation appear on both sides of bearing vibration frequency, and the continuous spectrum line appears near the meshing frequency as well. The increase of wear leads to the increase of transmission error amplitude, tooth back impact and the disappearance of side frequency bands on both sides of bearing vibration frequency. The main frequencies in the spectrum are meshing frequency and its high-order harmonic frequency, and the modulated sideband appears near the meshing frequency and its high-order harmonic.

INDEX TERMS Backlash, bearing radial clearance, comprehensive wearing capacity, meshing frequency, transmission error.

I. INTRODUCTION

The gear system is an elastic mechanical system consisting of a gear pair, a drive shaft, a bearing and a box. The gear motion state is related to the error excitation of the gear, the stiffness excitation and the movement of other components such as bearings [1]. Because of the existence of bearing clearance, the bearing will vibrate in the tooth plane, which changes the center distance of the gears, and then changes the backlash. Different bearing clearances have different effects on the vibration characteristics of the gearbox. Moreover, due to the long-term operation of the gear, the tooth surface will be worn, and the increase of wear will change the tooth profile error and the dynamic transmission error. The accumulation of wear will change the frequencies of gears. The modal analysis of worn gears can avoid the frequency migration zone caused by wear in the design of the gearbox, which has a positive effect on the design of gearbox.

The multi-gap coupling dynamic model of the gear-bearing system with backlash and bearing clearance has been deeply studied by many scholars. Qiu *et al.* [1] studied the dynamic characteristics of the planet gear from the aspects of modal characteristics, parameter instability and nonlinear dynamic response. Liu *et al.* [2] studied the dynamic response of the spur gear pair system and the interaction between bearing clearance and backlash. It is found that the clearance has self-adaptive characteristics, and the reduction of bearing center distance and the increase of input torque will lead to tooth squeezing. Li and Peng [3] used fractal theory to calculate the non-linearity of backlash and bearing clearance and carried out experimental verification. Xiang *et al.* [4] established a bending-torsion coupling dynamic model of bearing-rotor-gear system considering backlash, bearing clearance, eccentricity of gear teeth and time-varying stiffness, and studied

The associate editor coordinating the review of this article and approving it for publication was Jiajie Fan.

the coupling vibration relationship between bearing end and gear end. Zhu *et al.* [5] studied the chaotic, bifurcation characteristics and the strong coupling effect of the gap on the nonlinear behavior in the system under different backlash and bearing clearance of the planetary and sun gears. Zhang *et al.* [6] established a non-linear dynamic model of a composite planetary gear set with translational and torsional vibrations, and analyzed the comprehensive effects of meshing stiffness, backlash and bearing clearance on the load-sharing performance. Gou *et al.* [7] established a five-degree-of-freedom gear-rotor-bearing system dynamics model, and studied the influence of frequency, clearance, bearing clearance, comprehensive transmission error and stiffness on the non-linear dynamics of the system. Sheng *et al.* [8] studied the main parameters which may cause chaos and bifurcation, such as bearing clearance, backlash and excitation frequency, and proposed a proportional integral chaos control method which can effectively reduce chaos and suppress chaos. Zhang *et al.* [9] established a multi-clearance torsional vibration model of the gear considering the backlash and bearing clearance, and analyzed the coupling effect between backlash and bearing clearance and its influence on the steady state of the system.

Due to the existence of non-linear backlash function, the gear transmission system has a complex dynamic behavior. Theodossiades and Natsiavas [10] developed a suitable mechanical model taking into account the gear mesh backlash and static transmission error as well as the essential nonlinearities due to the bearing clearance and contact characteristics, and demonstrated the existence of quasi-periodic and chaotic long time response for selected combinations of the system parameters. Xiang *et al.* [11] established a nonlinear torsional model of a multistage gear transmission system which consists of a planetary gear and two parallel gear stages with time-varying meshing stiffness, comprehensive gear error and multi-clearance. Yoon and Kim [12] replaced the nonlinear function of the backlash with a smoothing function for avoiding the convergence problem caused by the discontinuity of the backlash, and verified the effectiveness and feasibility of the proposed method. Prajapat *et al.* [13] modeled and estimated the backlash in the gear transmission system by the unscented Kalman filter, and verified the effectiveness of the method under different working conditions. Yang *et al.* [14] analyzed the influence of the backlash between the sun gear and the involute planetary gear on the transmission accuracy and load carrying capacity. Zheng *et al.* [15] proposed a nonlinear dynamic equivalent model of a servo backlash gear system with time-varying meshing stiffness and backlash, and analyzed the influence of different parameters on the system resonant frequency. Yang *et al.* [16] took the planetary gear reducer as a research object, and established the dynamics model of the space manipulator considering the factors such as backlash and tooth profile error. The simulation results show that backlash will lead to the accumulation of positioning error of the manipulator. Xu *et al.* [17] established a rigid-flexible coupling model for rolling mill drive system considering the factors such as time-varying stiffness and backlash, and analyzed the vibration characteristics of the system under different backlash and rotation speed. Chen and Tang [18] studied the effects of friction, time-varying clearance and random clearance on the steady-state response of the gear system. Spitas and Spitas [19] analyzed the dynamic contact of gears starting from basic principles and derived an accurate analytical model for the coupling between the compliance, contact geometry, the backlash, and the torsional and lateral displacements and deflections in a general three-dimensional multi-DOF system.

In the gear transmission system, the gear meshing state is seriously affected by the bearing vibration. Liu *et al.* [20] considered that the wedge was a comprehensive effect of gravity, centrifugal force and clearance of planetary bearing. The gravity effect played a dominant role only at low rotating speed through numerical simulation. Shi *et al.* [21] established the dynamic model of a spur gear pair under multi-state meshing conditions, where time-varying meshing stiffness, time-varying friction, load distribution, comprehensive transmission error and backlash are included in the model. Fernandez-del-Rincon *et al.* [22] established a complex gear transmission model considering both internal and external excitation of gears and composite excitation of bearings. The meshing force of gears and contact force of bearings were calculated when the center distance of gears was changed due to bearing vibration. Gündüz *et al.* [23] established a comprehensive analysis model for the performance of high-speed input gear shaft bearings, and analyzed the influence of assembly-induced bearing clearance changes and uneven thermal expansion on the performance of bearings. Sawalhir and Randall [24] presented a simulation model for a gearbox test rig to simulate gear and bearing interactions, in which a range of bearing faults can be implemented.

Gear wear throughout its entire life cycle, and it is difficult to quantitatively describe the severity. Gear wear introduces geometric deviations in gear teeth and alters the load distribution across the tooth surface. Wear also increases the gear transmission error, generally resulting in increased vibration, noise and dynamic loads. Feng *et al.* [25] developed a vibration-based method to update a wear prediction model to monitor and predict the gear wear process. Shen *et al.* [26] divided the failure of planetary gears into two stages: slight wear and fatigue source generation. In the fatigue source generation stage, the roundness error of the inner surface and the profile error of the tooth surface will affect the radial clearance of the gear pair. Gao *et al.* [27] established a six-degree-of-freedom gear meshing coupling dynamics model, the dynamics characteristics of gear system with uniform wear of tooth surface and surface wear of eccentric gear were simulated. Li and Cui *et al.* [28] analyzed the effects of shaft cracks and tooth wear on the dynamic behavior of the system, and the interaction between crack and wear were analyzed. Janakiraman *et al.* [29] determined the wear coefficient under different working conditions and surface contact

conditions, and gave an empirical formula for estimating the wear coefficient. Brethee *et al.* [30] analyzed the effect of wear on the dynamics of gear transmission system, and processed the response signal of gear box in case of severe wear to verify the feasibility of the model and parameters. Prabhu Sekar and Sathishkumar [31] studied the effects of stiffness, pressure angle and transmission ratio of non-standard gears on wear. Wu *et al.* [32] calculated gear wear under static condition, obtained the backlash caused by wear, and analyzed the dynamic response of the gear system caused by wear.

In summary, many scholars have done a lot of valuable work on the research of side clearance, bearing clearance and gear wear. However, the research on multi-clearance gear system with wear is relatively few, or the Archard model is substituted into the model to simulate the interaction between wear and clearance, which will greatly increase the amount of simulation calculation, or the distribution of tooth surface wear is considered to be uniform, which is slightly different from the real distribution of wear.

In this paper, the triangular function is used to simulate the comprehensive wear distribution of a pair of meshing gears, and it is substituted into the gear system with multi-clearance to analyze the coupling effect. The lumped mass method is used to establish the torsional vibration model of the gear pair considering the tooth deformation, backlash, elastic support of the support system and tooth surface wear. This paper focuses on the effects of different backlash, bearing clearance and tooth surface wear on the dynamic response of the gear, and the dynamic transmission error and vibration severity of the gear with different degrees of wear. The structure of the paper is as follows: Section II gives a torsional vibration model of gear pair, and discusses the bearing radial clearance, dynamic backlash and motion differential equations and dimensionless; section III discusses the influence of parameters on dynamic characteristics of a gear system; Conclusions are given in Section VI.

II. GEAR SYSTEM MODELING

A. TORSIONAL VIBRATION MODEL OF GEAR PAIR

Figure 1 shows a pair of spur gear pair torsional vibration models established by the lumped mass method. The tooth deformation, damping, backlash and support system elasticity are considered in the system, and the coupling dynamic characteristics of the rotor are neglected. Six degrees of freedom of the system are introduced into the system, that is $\{d\} = \{\theta_1, \theta_2, x_1, x_2, y_1, y_2\}$. Where θ_1 and θ_2 are the rotational angular displacement of the driving and driven wheels; x_1 and x_2 are the lateral displacements of the driving and driven wheels; y_1 and y_2 are the radial displacements of the driving and driven wheels.

The following assumptions were made in this paper:

1) The gearbox body is rigid and does not deform. The gears and bearings are linear elastomers. The installation error of each fitting is neglected. The transmission shaft is rigid and there is no bending and torsion deformation.

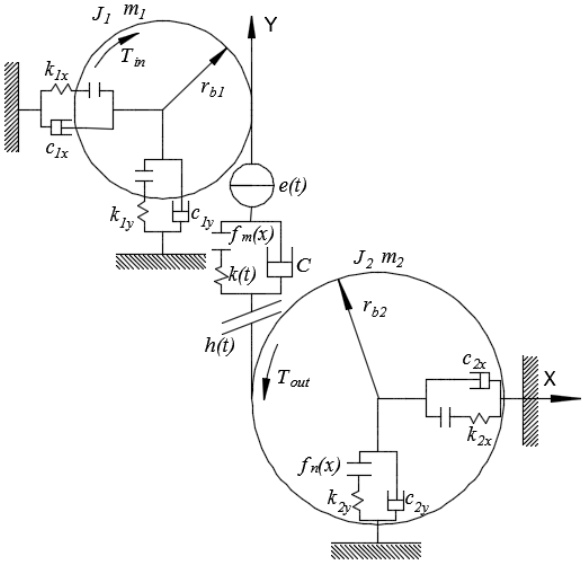

FIGURE 1. Torsional vibration model of a pair of spur gears.

2) Torsional vibration of meshing gear pair is only carried out around Z axis in its own plane, and radial vibration exists in X and Y directions.
3) The friction between the teeth is neglected.
4) The gravity of each component is neglected.

In Figure 1, J_1 and J_2 is the moment of inertia of the driving wheel and the driven wheel respectively. m_1 and m_2 is the mass of the driving wheel and the driven gear respectively. $f_m(x)$ and $f_n(x)$ are non-linear functions of backlash and clearance. r_{b1} and r_{b2} are the driving wheel and the driven wheel radius of the base circle. k_{ix} and k_{iy} $(i = 1, 2)$ is the average stiffness of the support on the driving wheel and the driven wheel bearings in X and Y direction respectively. c_{ix} and c_{iy} $(i = 1, 2)$ are the damping parameters on the X and Y direction corresponding bearing. T_{in} and T_{out} are the input and output torque. $h(t)$ is the comprehensive wear of the gear pair. $e(t)$ is the comprehensive meshing error. $K(t)$ is the time-varying comprehensive meshing stiffness. C is the damping coefficient.

B. BEARING RADIAL CLEARANCE

Because of the clearance between the inner ring and the outer ring of the bearing, the radial runout between the rotor and the outer ring occurs when the system runs, which is expressed by the clearance vector. The components of clearance vectors of the main and driven wheel bearings in X and Y directions are x_i, and y_i $(i = 1, 2)$.

The vibration displacement component x_i and y_i $(i = 1, 2)$ and the bearing initial clearance b_n are used to describe the deformation of the contact between the rigid bodies of the bearing. The deformation function $f_n(x_i)$ is expressed as:

$$f_n(x_i) = \begin{cases} x_i - b_n & x_i > b_n \\ 0 & |x_i| \le b_n \\ x_i + b_n & x_i < -b_n \end{cases} \tag{1}$$

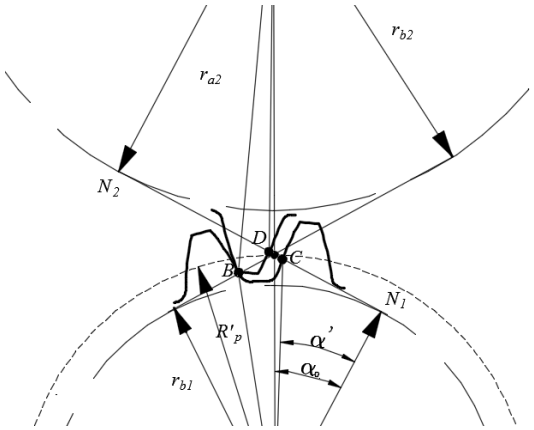

FIGURE 2. Schematic diagram of dynamic backlash.

In Eq. (1), when $|x_i| > b_n$, the inner ring is in contact state and is subjected to contact force. The direction of the force depends on the direction of x_i, and the magnitude of the force depends on the value of $|x_i \pm b_n|$. When $|x_i| \leq b_n$, the rotor and bearing are in free motion or critical state, and the contact force is zero, and the bearing inner ring is not affected by outer ring and ball force.

C. DYNAMIC BACKLASH

The backlash exists in the meshing gear pair, and it's closely related to the machining accuracy of the gear teeth. Backlash plays an important role in the gear system, which can prevent the gear teeth from being blocked by thermal expansion and contraction due to friction heating. The lubricating oil can be stored between the teeth to form a lubricating oil film, which can improve the boundary conditions of the contact surface and slow down the wear. Appropriate backlash is conducive to the normal operation of the gears. Excessive backlash will aggravate the collision between the teeth and generate large vibration and noise [4].

Gear vibration will cause the displacement response of the bearing in the radial and tangential plane, change the center distance of the two wheels, and then lead to the change of the backlash of the gear teeth. In this paper, the gear meshing principle is analyzed, and the expression of dynamic backlash is obtained by taking the actual meshing angle as a variable. Figure 2 shows the meshing diagram of a pair of standard gears. Point B is the meshing point on the line of action, and points C and D coincide when the gears mesh.

When the standard gears are installed, the straight line distance between the common tangent of the base circle and the intersection point C and D of the involutes of the main and driven wheels is the initial backlash. When the gear vibrates, both the main and the driven wheels will vibrate in X and Y directions, which will makes the actual center distance and meshing point change. Through geometric calculation, the actual meshing angle and the actual meshing radius of the base circle can be obtained, and then the actual meshing point tooth spacing can be calculated. The tooth spacing subtracts the difference between the tooth thickness of the main and driven wheels, multiplies the cosine value of the actual pressure angle, and adds the initial backlash to get the dynamic backlash.

Because of the radial runout of the bearing caused by clearance, points C and D do not coincide, and the actual center distance a' is not equal to the theoretical center distance a_0. At this time, the actual center distance a' and the actual pressure angle α' can be expressed as:

$$a' = \sqrt{\begin{matrix}(a_0 \cos\alpha_0 + x_2 - x_1)^2 \\ +(a_0 \sin\alpha_0 + y_1 - y_2)^2\end{matrix}} \tag{2}$$

$$\alpha' = \arccos\left(\frac{a_0}{a'}\cos\alpha_0\right) \tag{3}$$

On the common tangent line N_1N_2 of the gear base circle, the dynamic backlash value can be expressed as $|CD|$:

$$\begin{aligned}|CD| &= 2b'_c \\ &= (2\pi R'_p/Z_1 - s'_1 - s'_2)\cos(\alpha') + 2b_c\end{aligned} \tag{4}$$

where R'_p is the nodal radius in actual meshing. s'_1 and s'_2 is tooth thickness of the main and driven wheel respectively. Z_1 is the number of the driving gear teeth, and $2b_c$ is the initial tooth backlash.

According to Eq. (3) and Eq. (4), the relationship between the dynamic half-backlash and the actual center distance is:

$$b'_c = a_0 \cos\alpha_0 \left(inv\alpha' - inv\alpha_0\right) + b_c \tag{5}$$

The role of backlash in gear transmission is complex and difficult to be expressed by simple linear function. Kahraman *et al.* [33] use piecewise function to describe its behavior.

$$f[f_x(t)] = \begin{cases} f_x(t) - b'_c & f_x(t) \geq b'_c \\ 0 & -b'_c < f_x(t) < b'_c \\ f_x(t) + b'_c & f_x(t) \leq -b'_c \end{cases} \tag{6}$$

where $f_x(t)$ is the dynamic transmission error along the meshing line. When $f_x(t)$ is greater than or equal to b'_c, the gear is in the normal meshing state. When $f_x(t)$ is less than b'_c and greater than $-b'_c$, the gear is in the disengaged state, and the dynamic meshing force is zero. When $f_x(t)$ is less than or equal to $-b'_c$, a back impact occurs at this time.

D. EQUATION OF MOTION

According to Figure 1, the differential equation of the system motion is established as follows.

$$\begin{cases} J_1\ddot{\theta}_1 + r_{b1}C\dot{f}_x(t) + r_{b1}K(t)f_m\left[f_x(t)\right] = T_{in} \\ m_1\ddot{x}_1 + C_{1x}\dot{x}_1 + k_{1x}f_n(x_1) = F_{x1} \\ m_1\ddot{y}_1 + C_{1y}\dot{y}_1 + k_{1y}f_n(y_1) + K(t)f_m\left[f_x(t)\right] + C\dot{f}_x(t) = F_{y1} \\ J_2\ddot{\theta}_2 + r_{b2}C\dot{f}_x(t) + r_{b2}K(t)f_m\left[f_x(t)\right] = -T_{out} \\ m_2\ddot{x}_2 + C_{2x}\dot{x}_2 + k_{2x}f_n(x_2) = -F_{x2} \\ m_2\ddot{y}_2 + C_{2y}\dot{y}_2 + k_{2y}f_n(y_2) - K(t)f_m\left[f_x(t)\right] - C\dot{f}_x(t) = -F_{y2} \end{cases} \tag{7}$$

where F_{x1}, F_{y1}, F_{x2} and F_{y2} are the pre-tightening forces of the driven wheel in the X and Y directions.

$$f_x(t) = \theta_1 r_{b1} - \theta_2 r_{b2} - e(t) - y_1(t) + y_2(t) - h(t) + (x_2 - x_1)\cos(\theta_x) \quad (8)$$

where $f_x(t)$ is the gear dynamic transmission error. In addition to introducing torsional vibration displacement and static transmission errors of the main and driven wheels, it also considers the vibration displacement $y_1(t)$ and $y_2(t)$ of the bearing in Y direction, the displacement component $(x_2 - x_1)\cos(\theta_x)$ of the bearing in the X direction along the center distance, and the total wear of the tooth surface $h(t)$.

$e(t) = e_m \cos(w_e t)$ is the static transmission error. w_e is the meshing frequency. θ_x is the angle between the X axis and the gear center distance line. $h(t) = h_m |\cos(w_e t/2)|$ is the gear pair comprehensive wear amount, and h_m is the wear amount amplitude.

Introducing the time nominal scale $\tau = w_n t$, the natural frequency of the system is $w_n = \sqrt{K_m/m_e}$, and m_e is the effective quality of the gear. $m_e = J_1 J_2/(J_1 r_{b2}^2 + J_2 r_{b1}^2)$, $\bar{x}_i = x_i/b_c$, $\bar{y}_i = y_i/b_c$, $\bar{f}_x(t) = f_x(t)/b_c$, $(i = 1, 2)$, $w_h = w_e/w_n$. The dimensionless differential equations of the system are obtained by dimensionless treatment of the equations as follows:

$$\begin{cases} \ddot{\bar{f}}_x(\tau) = F_m + \ddot{\bar{y}}_1 - \ddot{\bar{y}}_2 + \cos(\theta_x)(\ddot{\bar{x}}_2 - \ddot{\bar{x}}_1) \\ -\bar{K}(\tau)\bar{f}_m\left[\bar{f}_x(\tau)\right] - 2\xi\dot{\bar{f}}_x(\tau) \\ -w_h^2 \bar{e}\sin(w_h\tau) - \ddot{\bar{h}}(\tau) \\ \ddot{\bar{x}}_1 = f_{1x} - 2c_1\xi_1\dot{\bar{x}}_1 - 2k_1k_{n1}\bar{f}_n(\bar{x}_1) \\ \ddot{\bar{y}}_1 = f_{1y} - 2c_2\xi_1\dot{\bar{y}}_1 - 2k_2k_{n1}\bar{f}_n(\bar{y}_1) - \bar{K}_1(\tau)\bar{f}_m\left[\bar{f}_x(\tau)\right] \\ -2\xi_1\dot{\bar{f}}_x(\tau) \\ \ddot{\bar{x}}_2 = -f_{2x} - 2c_3\xi_2\dot{\bar{x}}_2 - 2k_3k_{n2}\bar{f}_n(\bar{x}_2) \\ \ddot{\bar{y}}_2 = -f_{2y} - 2c_4\xi_2\dot{\bar{y}}_2 - 2k_4k_{n2}\bar{f}_n(\bar{y}_2) - \bar{K}_2(\tau)\bar{f}_m\left[\bar{f}_x(\tau)\right] \\ +2\xi_2\dot{\bar{f}}_x(\tau) \end{cases} \quad (9)$$

In the equation, the dimensionless damping coefficients are:

$$c_1 = c_{1x}/C, \quad c_2 = c_{1y}/C, \; c_3 = c_{2x}/C, \; c_4 = c_{2y}/C, \quad \xi = C/2m_e w_n, \quad \xi_i = C/2m_i w_n (i = 1, 2).$$

The dimensionless stiffness factors are:

$$k_1 = k_{1x}/K_m, \quad k_2 = k_{1y}/K_m, \; k_3 = k_{2x}/K_m, \; k_4 = k_{2y}/K_m, \; k_{ni} = K_m/(2m_i w_n^2)(i = 1, 2).$$

Other dimensionless parameters are:

$$F_m = T_{in}/r_{b1} m_e b_n w_n^2, \; \bar{e} = e/b_c, \; \bar{K}(\tau) = K(\tau)/m_e w_h^2, \; \bar{h}_m = h_m/b_c, f_{ix} = F_{xi}/m_i b_c w_n^2, \; f_{iy} = F_{yi}/m_i b_c w_n^2 (i = 1, 2), \; \ddot{\bar{h}}(\tau) = -w_h^2 \bar{h}_m |\cos(w_h\tau/2)|/4.$$

In order to make the time-varying stiffness in each cycle continuous and ease to calculate, the time-varying stiffness can be expressed as:

$$K(t) = K_m + K'_m \cos(w_e t) \quad (10)$$

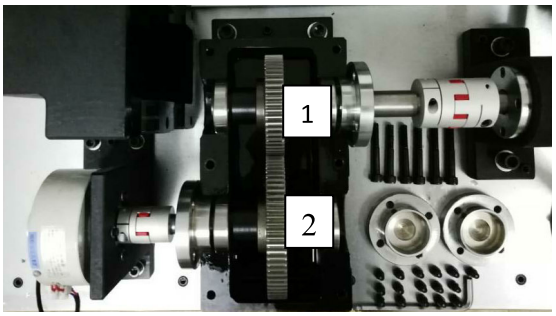

FIGURE 3. Gear box structure.

TABLE 1. Gear pair parameters.

Parameter name	Main wheel	Driven wheel
Number of teeth Z	55	75
Modulus m/mm	2	2
Pressure angle φ / °	20	20
Tooth width B/ mm	20	20
Roughness R_a/ μm	0.2	0.2
Tip height factor h_a^*	1	1
Top coefficient c^*	0.25	0.25

where K_m is the average of the time-varying comprehensive meshing stiffness, and K'_m is the stiffness amplitude.

Damping C is an important parameter affecting the dynamic characteristics of the gear [34]:

$$C = 2\xi_p \sqrt{\frac{K_m J_1 J_2}{r_{b1}^2 J_2 + r_{b2}^2 J_1}} \quad (11)$$

where ξ_p is the meshing damping ratio of the gear, and is generally between 0.03-0.17.

III. THE INFLUENCE OF PARAMETERS ON DYNAMIC CHARACTERISTICS OF A GEAR SYSTEM

A. GEARBOX SYSTEM

The spur gear of the gearbox shown in Figure 3 is taken into account. The main wheel 1 meshes with the driven wheel 2 and the inner hole of the gear and the shaft are often connected by interference fit, axial fixation of gears by shaft shoulder and sleeve. The circumferential direction is fixed by the key and the keyway, so that the gear can only rotate along the axis. Deep groove ball bearings are installed at both ends of gear shaft. The gear speed is controlled by applying load to quantify the speed of the gear as the applied load. Table 1 shows the specific parameters of the meshing gear pair.

B. THE INFLUENCE OF BEARING CLEARANCE ON THE STEADY STATE OF THE SYSTEM

In the gear system, considering the bearing clearance will complicate the dynamic characteristics and affect the steady-state response characteristics of the system. Taking the Y direction vibration displacement response of the driving

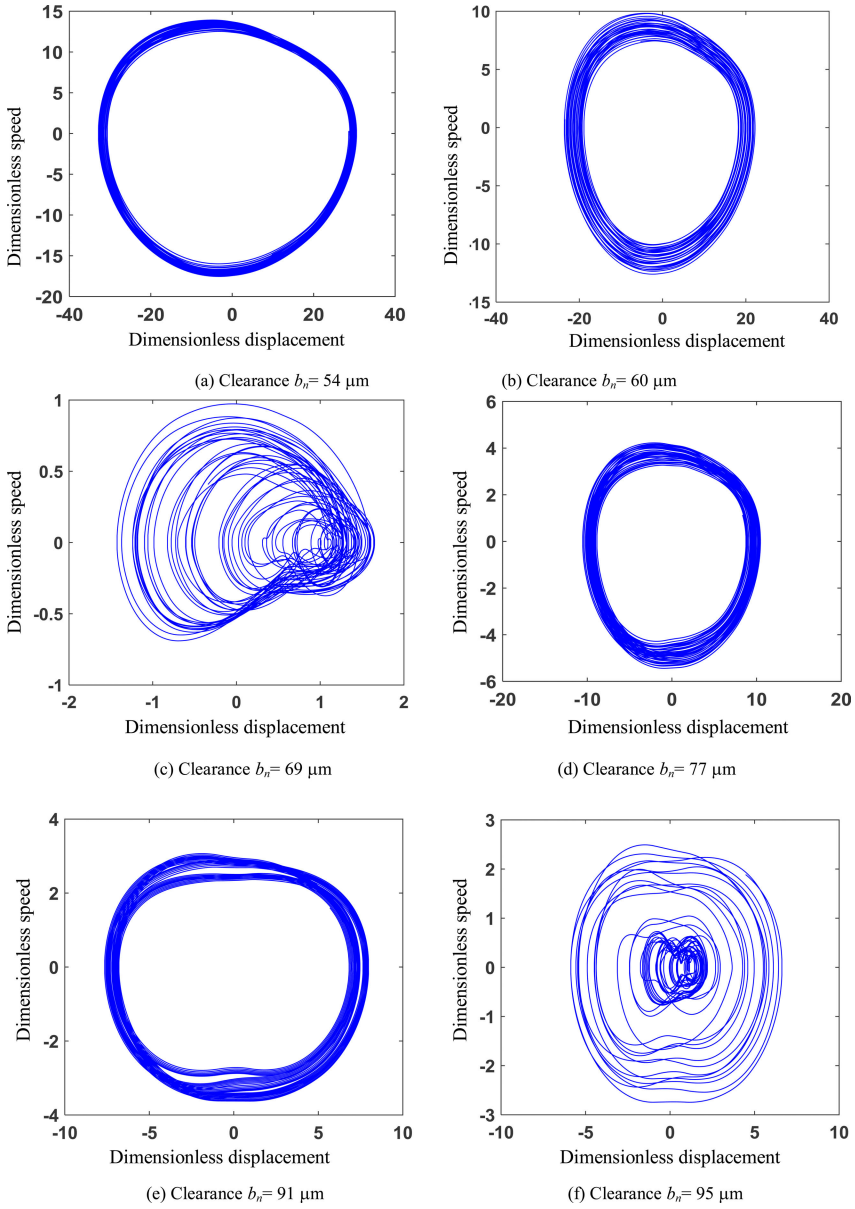

FIGURE 4. Phase diagram for different clearances.

wheel as an example, the influence of different clearance on the dynamic behavior of the system is analyzed.

In this paper, 6205 deep groove ball bearing is used in the gear box system. Because the internal and external rings of the bearing and the rolling body are worn and the clearance is increased, the specific clearance can be obtained by measuring the plug gauge, and the clearance can be controlled by the service time of the bearing. To solve the problem of bearing loosening failure, we can increase lubricating grease, clean up the dirt in the journal, replace the bearing end cap, and replace the bearing if the loosening failure can not be alleviated.

Depending on the bearing selected, the recommended bearing clearance range is 40 μm to 64 μm. In order to cover the normal range and to study the steady-state response when the normal range is exceeded, the range is set to 50 μm -100 μm.

Under different bearing clearances, the vibration periodicity and trend of the driving and driven wheels are identical. The dynamic response of the driving wheel is shown in Figure 4. With the change of bearing clearance, the dynamic response presents different states: when clearance $b_n = 54\mu$m, the vibration response is a single period. With the increase of clearance, the vibration response

TABLE 2. Response results under different clearances.

Clearance (μm)	Maximum radial dimensionless displacement	Maximum radial dimensionless velocity	Vibration Periodicity
51	30.7	14.4	Quasi-periodic
55	29.9	13.6	Periodic
60	23.1	10.3	Quasi-periodic
66	1.8	0.82	Chaotic
78	10.3	4.2	Quasi-periodic
80	2.0	1.1	Chaotic
81	9.7	3.8	Quasi-periodic
87	2.1	0.9	Chaotic
93	7.4	2.9	Double-periodic
100	2.2	0.7	Chaotic

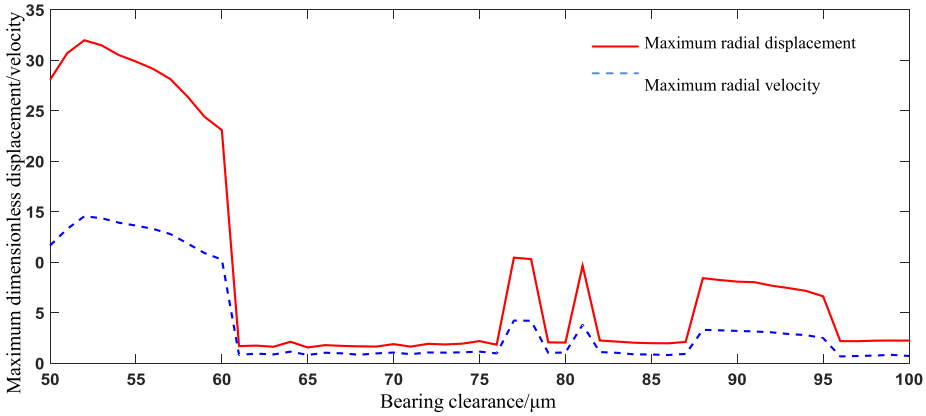

FIGURE 5. Maximum dimensionless displacement and velocity diagram of different bearing clearances.

experiences quasi-period, chaotic, quasi-periodic, double-periodic and chaotic.

In the phase diagram of Figure 4, if it is a circle, the system is periodic under this condition. When the phase diagram shows a finite number of circles, the system is double-periodic under this condition. When a circular ring is shown in the phase diagram, the system is quasi-periodic under this condition. When the phase diagram shows irregular lines, it shows that the system is chaotic under this condition.

Figure 4 shows that the bearing does not move around the central axis, but simply moves harmonically in the Y direction in some cases. The meshing force of the meshing gear pair is an important reason for the motion of the gear. In addition, due to the impact of damping and bearing inner and outer rings, a corresponding force will be generated to balance the force. The relationship between the velocity of Y axis and the distance of X axis is drawn to illustrate the periodicity of the bearing under this clearance.

The vibration response of the gear under different bearing clearances is listed in Table 2. It can be seen that from Table 2, although the bearing clearance has only a slight change, the vibration periodicity is completely different, reflecting the characteristics of the non-autonomous system. In addition, the maximum displacement and velocity values of the vibration are also very different, and the specific trend is shown in Figure 5.

It can be seen that from Figure 5, as the bearing clearance increases, the variation trend of maximum radial displacement and velocity is similar. When the clearance value is 50 μm - 60 μm, 77 μm - 78 μm, 81 μm and 88 μm - 95 μm, the vibration periodicity is a period, double-periodic or quasi-periodic. When the clearance value is between 50 μm and 60 μm, the system state gradually changes from periodic to quasi-periodic, and the maximum displacement and velocity are larger, with a slight slowdown trend. When the clearance value is between 77 μm and 78 μm and 81 μm, the system is in quasi-periodic state, and its maximum displacement and velocity have been greatly reduced compared with before, but it is still large compared with the chaotic state, reflecting a step of the system. When the clearance value is between 88 μm and 95 μm, the system enters a doubled periodic state, and the maximum displacement and velocity decrease slightly. Generally speaking, the more obvious the periodicity of the system is, the larger the response range will be.

At this time, the maximum dimensionless displacement and velocity are larger than those in chaos. When the vibration periodicity is chaotic, the values of displacement and velocity are relatively small, maintaining a relatively stable

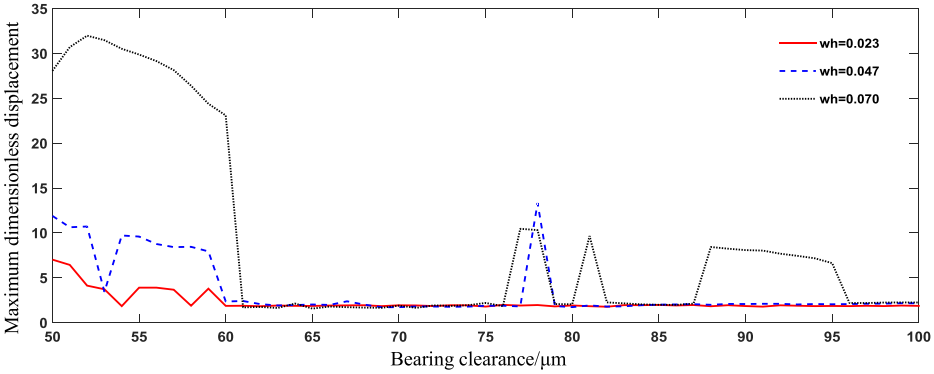

FIGURE 6. Maximum dimensionless displacement at different excitation frequencies.

value, the clearance has little effect on the vibration amplitude. In addition, the steady-state response of the driven wheel also conforms to this rule.

The maximum displacement response at high speed $1500r/\min(w_h = 0.07)$ has been calculated. In order to further study the influence of bearing clearance on displacement response, we simulate the steady-state response of the system with different dimensionless excitation frequencies (rotational speeds) and different clearances. The result is shown in Figure 6.

Figure 6 shows the maximum displacement response of the bearing at different excitation frequency. When the excitation frequency $w_h = 0.047$ (the rotational speed is 1000 r/min) and the clearance is in the range of 50 μm - 60 μm, the maximum displacement response is large and unstable. A step phenomenon occurs when the clearance is 78 μm. When the excitation frequency $w_h = 0.023$ (the rotational speed is 500 r/min) and the clearance is in 50 μm - 60 μm, the maximum displacement response changes slightly, and after the clearance is 60 μm, the maximum displacement response is relatively stable, and is not affected by the clearance.

It can be seen that the clearance has a great influence on the periodicity of the vibration response of the gear system at high speed. With the increase of clearance, the system will traverse a variety of states without regularity and alternating. When the system is in a periodic state, the maximum displacement response is often larger than that in a chaotic state, and there is a step phenomenon. It can be seen that the smaller the excitation frequency of the system is, the smaller the influence of clearance on the maximum displacement response is. For the gear system selected in this paper, the clearance is more suitable for 60 μm - 75 μm.

C. CORRESPONDING EFFECTS OF THE BACKLASHP ON THE STEADY STATE OF THE SYSTEM

The backlash is one of the important variables that affect the dynamic response of the gear system. Taking the Y-direction vibration displacement response of the driving wheel as an example, the dynamic response of the system with different initial backlash sizes is solved, and the influence of different initial backlash values on the system vibration is analyzed. Figure 7 shows the phase diagrams of six different backlashes.

It can be seen that from Figure 7, with the change of backlash, the system traverses multiple states, such as double-period, quasi-period, chaos and period. From the maximum abscissa of six phase diagrams, it can be seen that with the increase of backlash, the vibration amplitude of the gear in the Y direction increases, which aggravates the vibration of the gear. This is because the increase of backlash makes the meshing impact between the gear teeth intensify, and the meshing force transfers to the bearing part, which aggravates the vibration. Table 3 shows the maximum dimensionless displacement and velocity of the system under each clearance.

Also, it can be seen that from Figure 4 and Figure 7, with the increase of bearing clearance, the process from a single circle to a ring, multiple (finite) rings and complex infinite lines appears in the phase diagram. It shows that the system traverses periodic, quasi-periodic, doubled periodic and chaotic states. When the abscissa values of phase diagrams change considerably, a step phenomenon appears. Backlash enlargement is similar, but the order of traversing states may be different.

The dynamic transmission error of the gear system with different backlash is simulated and calculated, as shown in Figure 8. The vibration amplitude of transmission error increases with the increase of the backlash. When the backlash $b_c = 50\mu$m, the amplitude is small, and the tooth detachment occurs, which is a chaotic state. When the backlash $b_c = 100$ μm, the amplitude becomes larger and slight backlash occurs. When the backlash is further enlarged, the amplitude increases obviously, and the impact on the back of the teeth becomes more obvious. The system changes from chaos to quasi-periodic state.

Figure 9 shows the spectrum with different backlashes. w_h is the gear meshing frequency, and w_n is the bearing variable stiffness vibration frequency. With the increase of backlash, the amplitude increases. The continuous spectrum

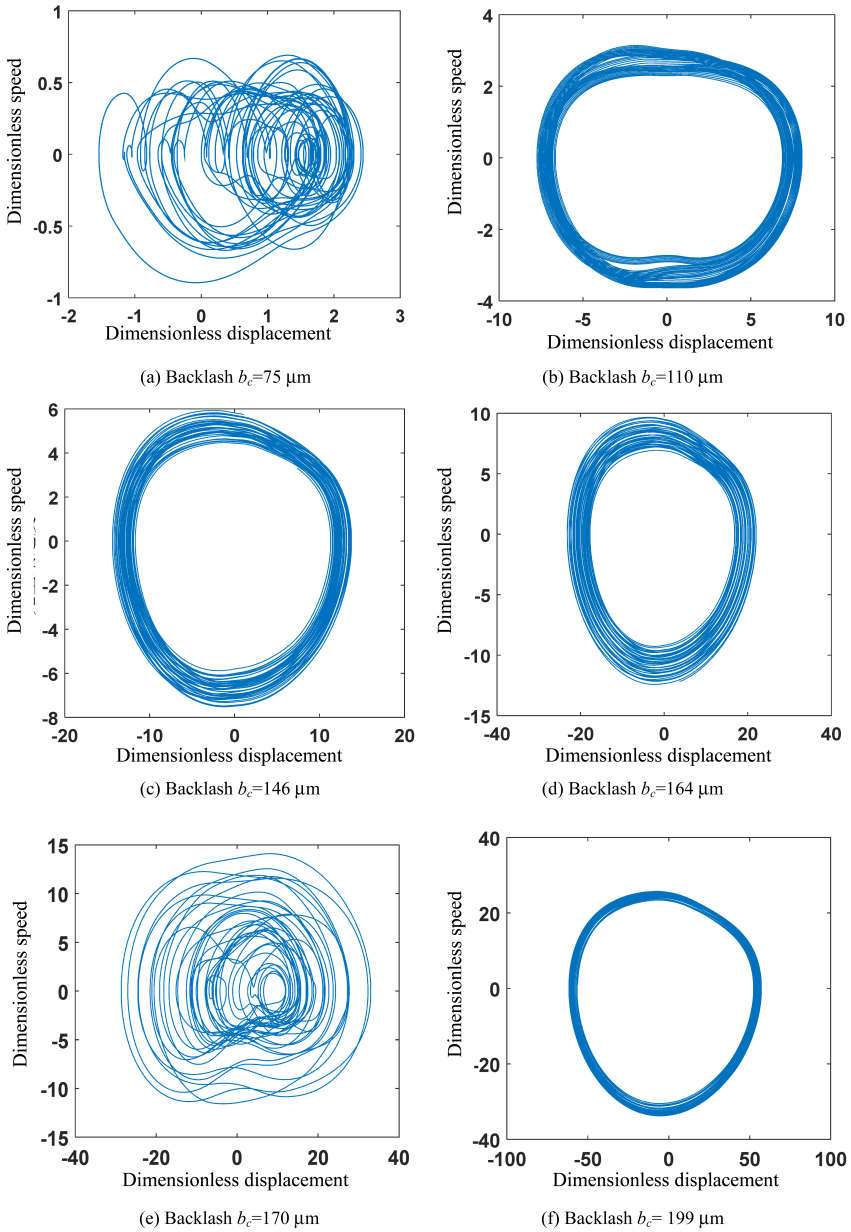

FIGURE 7. Phase diagram for different backlash.

TABLE 3. Response results under different backlash.

Backlash (μm)	Maximum radial dimensionless displacement	Maximum radial dimensionless velocity	Vibration periodicity
75	2.57	0.67	Chaotic
110	8.0	3.14	Double-periodic
125	9.8	3.9	Quasi-periodic
131	10.4	5.2	Chaotic
146	12.5	5.9	Quasi-periodic
164	22.0	9.6	Quasi-periodic
170	32	15	Chaotic
199	57.2	25.7	Periodic

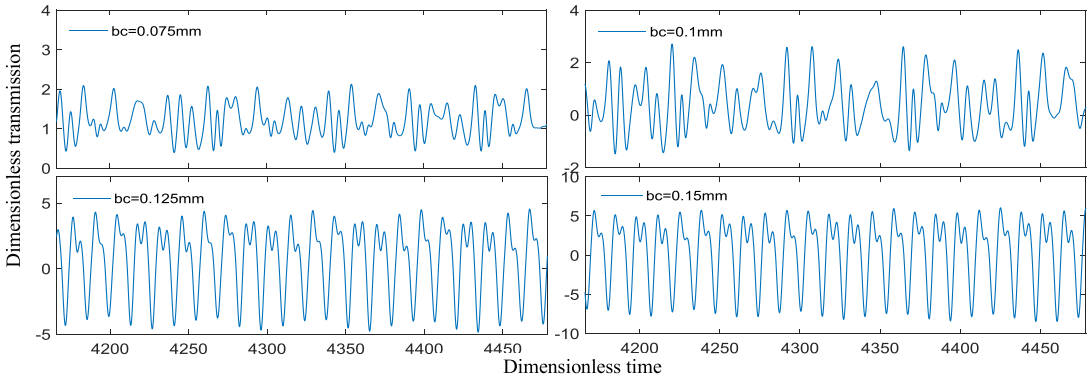

FIGURE 8. Dynamic transmission error response with different backlash (clearance $b_n = 100\mu$m).

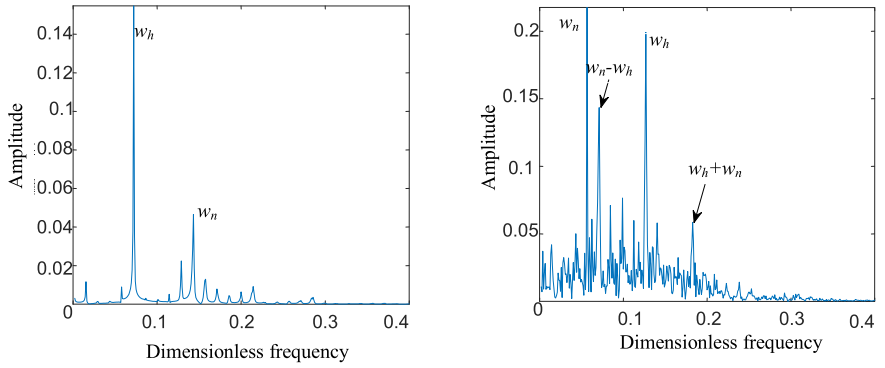

(a) Spectrum at backlash b_c=50μm

(b) Spectrum at backlash b_c=100μm

FIGURE 9. Spectrum under different backlash.

lines appear near the meshing frequency, and the vibration signals become more complex. When backlash $b_c = 100\ \mu$m, the side frequency band generated by amplitude modulation appears on both sides of bearing vibration frequency. The influence of backlash nonlinearity on the system increases, and the vibration becomes more complex and intense.

D. IMPACT OF COMPREHENSIVE WEAR

As the running time of gear system becomes longer and longer, the wear of meshing gear pair increases gradually. There is almost no wear at the pitch joints of teeth with wear faults gear, and the most serious wear is near the root and top of the teeth. Trigonometric function is used to simulate the comprehensive wear of meshing gear pairs. With the change of the pressure angle at the meshing point, the maximum wear of single tooth is obtained at the root of the tooth. When the tooth is meshed in or out, the root of the main gear is meshed at the top of the driven gear and the other engaged gear teeth are disengaged at the root of the driven gear teeth. Assuming that there is no wear or little wear near the pitch point, it can be neglected. If the pressure angle of the joint is equal to half of the sum of the maximum pressure angle and the minimum pressure angle, the expression of the comprehensive wear gauge is calculated from Archard's formula as follows:

$$h(\tau) = h_m \left|\cos(w_h \tau/2)\right| \tag{12}$$

where h_m is the superposition of the wear of the tooth top and the tooth root of the meshing gear.

According to the meshing principle of the gear teeth, the wear values of the main and driven wheels are added up with the meshing angle as a variable, and the comprehensive wear values of the gear pairs varying with the meshing points are obtained. Eq. (12) is obtained after dimensionless treatment of time scale $\tau = w_n t$.

Eq. (12) is used to express the comprehensive wear of the tooth surface in a meshing period. By doing so, the calculation process can be simplified and the quantitative relationship between the comprehensive wear of the tooth surface and the clearance of the tooth side can be quickly calculated.

The backlash of different meshing points is different, so the time-varying half-tooth backlash is:

$$b_c{}' = a_0 \cos\alpha_0(\mathrm{inv}\alpha' - \mathrm{inv}\alpha_0) + b_c + h_m \left|\cos(w_h \tau/2)\right|/2 \tag{13}$$

Defined that the maximum comprehensive wear amount h_m ($h_m = 200\ \mu$m) is 2 times of the initial half clearance,

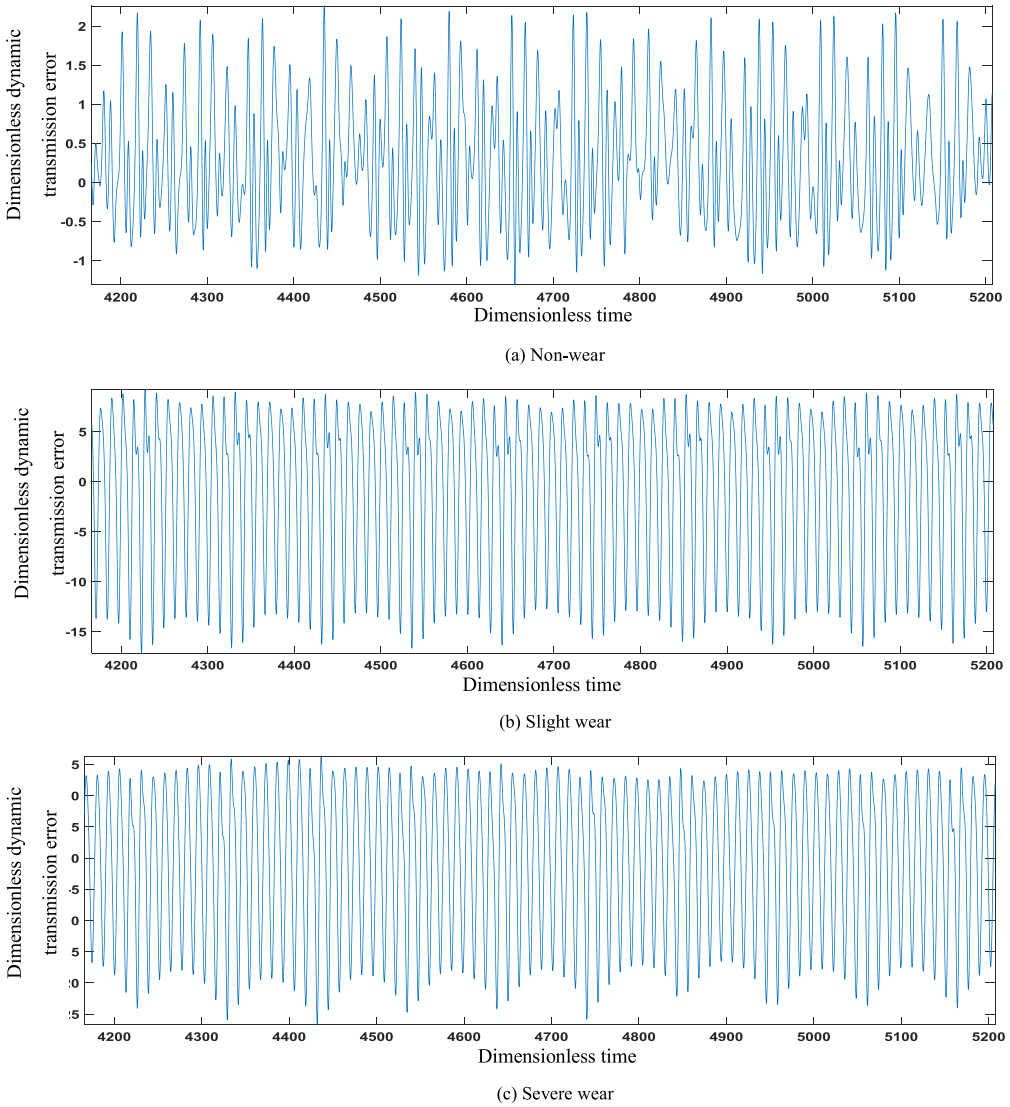

FIGURE 10. Dynamic transmission error time displacement response diagrams under different wear conditions.

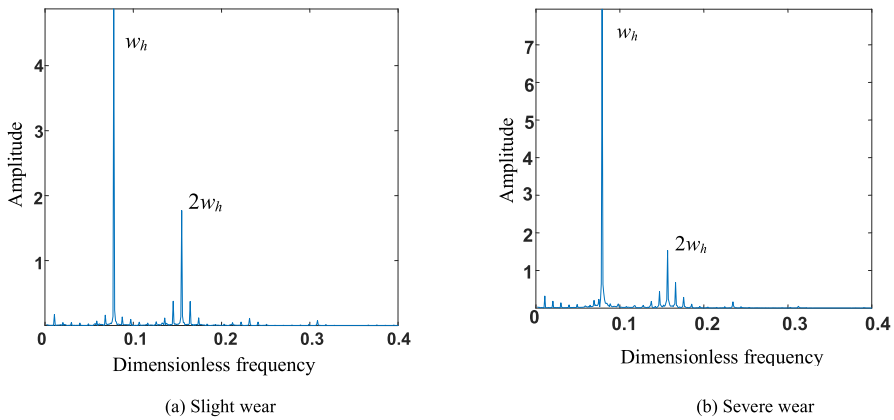

FIGURE 11. Spectrogram in different wear states.

slight wear occurs on the gears. The maximum comprehensive wear amount h_m ($h_m = 500\ \mu$m) is 5 times of the initial half clearance, severe wear occurs on the gears, and the maximum comprehensive wear amount $h_m = 0$, and there is non-wear. The time-domain response of dynamic transfer error is obtained by numerical simulation of non-wear, slight wear and severe wear, respectively, the corresponding spectrum is shown in Figure 10 and 11.

When there is no wear, the system is in chaotic motion state, and the mean value of transmission error is low. The gear teeth appear tooth detachment and slight back impact. When wearing slightly or severely, the system enters the period from chaos, and the magnitude of transmission error increases. Wear also makes the side bands of bearing vibration frequency disappear without wear. The main components of the spectrum are meshing frequency and its high-order harmonic frequency, and the modulated side band appears near it. When the wear is severe, the spectrum is similar to that of slight wear, but severe wear makes the peak value of spectrum signal higher and the characteristic signal more obvious. In addition, the increase of wear makes the backlash increase, which makes the backlash of teeth collide more intensely, and accelerates the wear process forward.

IV. CONCLUSION

1) With the increase of clearance, the system traverses many states, such as period, double-period, quasi-period and chaos. When the clearance is in the range of 50 μm - 60 μm, the system vibration is greatly affected by the clearance. When the gears rotate at high speed, the maximum displacement response of the system appears a step phenomenon, but the degree of the response tends to slow down. At medium and low speeds, the step phenomenon disappears, and bearing clearance has little effect on gear vibration.
2) With the increase of backlash, the amplitude of dynamic transmission error increases, and the gear system starts from normal meshing to a slight backlash. With the further increase of backlash, the amplitude and meshing force increase obviously, and the impact on the back of teeth becomes more and more intense. In addition, when the backlash increases from 50 μm to 100 μm, the side band of bearing vibration frequency caused by amplitude modulation appears. The spectrum around the meshing frequency becomes continuous and the vibration signal becomes more complex. The non-linearity of backlash has great influence on the steady state of the system, and the vibration is more complex and violent.
3) When there is no wear, the system is chaotic and the amplitude of dynamic transfer error is small. With the increase of wear, the amplitude of dynamic transmission error increases, the back impact of teeth occurs, and the meshing force between teeth increases correspondingly, which aggravates the wear process. Wear also make the sidebands on both sides of the bearing vibration frequency disappear when wear is not occurring. The main frequency in the spectrum is meshing frequency and its high-order harmonic frequency. The modulation sideband appears on both sides of the meshing frequency and its higher harmonic frequency.
4) According to the wear distribution of the tooth profile, the wear values of the main and driven wheels are added together to obtain the comprehensive wear values of the gear pairs varying with the meshing points, and the triangular function is used to simulate the comprehensive wear values of a pair of meshing gear pairs. This method can simplify the calculation and conveniently obtain the change of the backlash caused by wear. The results show that the simulation effect is very good and accords with the actual situation.
5) In order to simplify the calculation, triangular function is used to simulate the wear of gears. The node is set between the maximum pressure angle and the minimum pressure angle, which is slightly different from the actual situation. In addition, this paper does not take into account the reciprocating wear of meshing points caused by gear installation error and bearing clearance, which makes the wear amount near the joint not zero, nor does it take into account the wear distribution along the tooth width direction, which needs to be further studied.

REFERENCES

[1] X. H. Qiu, Q. K. Han, and F. L. Chu, "Review on dybnamic analysis of wind turbine geared transmissin systems," *J. Mech. Eng.*, vol. 50, no. 11, pp. 23–36, Jun. 2014.
[2] Z. Liu, Z. Liu, J. Zhao, and G. Zhang, "Study on interactions between tooth backlash and journal bearing clearance nonlinearity in spur gear pair system," *Mech. Mach. Theory*, vol. 107, no. 1, pp. 229–245, Jan. 2017.
[3] Z. X. Li and Z. Peng, "Nonlinear dynamic response of a multi-degree of freedom gear system dynamic model coupled with tooth surface characters: A case study on coal cutters," *Nonlinear Dyn.*, vol. 84, no. 1, pp. 271–286, Apr. 2016.
[4] L. Xiang, Y. Jia, X. Gao, W. Di, and Y. Li, "Effects of backlash on bending-torsion coupled vibration of a gear-rotor bearing system," *J. Vib. Shock*, vol. 35, no. 21, pp. 1–8, Nov. 2016.
[5] R. Zhu, D. Sheng, F. Lu, M. Li, and H. Bao, "Modeling and bifurcation characteristics of double stage planetary gear train with multiple clearances," in *Proc. ASME Des. Eng. Tech. Conf.*, vol. 10, Boston, MA, USA, Aug. 2015, Art. no. V010T11A017.
[6] H. Zhang, S. Wu, and Z. Peng, "A nonlinear dynamic model for analysis of the combined influences of nonlinear internal excitations on the load sharing behavior of a compound planetary gear set," *Proc. Inst. Mech. Eng., C, J. Mech. Eng. Sci.*, vol. 230, nos. 7–8, pp. 1048–1068, Jul. 2015.
[7] X. Gou, L. Zhu, and C. Qi, "Bifurcation and chaos analysis of a gear-rotor-bearing system," *J. Theor. Appl. Mech.*, vol. 56, no. 3, pp. 585–599, 2018.
[8] L. Sheng, W. Li, Y. Wang, M. Fan, and X. Yang, "Nonlinear dynamic analysis and chaos control of multi-freedom semi-direct gear drive system in coal cutters," *Mech. Syst. Signal Process*, vol. 116, no. 1, pp. 62–77, Feb. 2019.
[9] H. B. Zhang, R. Wang, Z. K. Chen, C. Wei, Y. Zhao, and B. D. You, "Nonlinear dynamic analysis of a gear-rotor system with coupled multi-clearance," *J. Vib. Shock*, vol. 34, no. 8, pp. 144–150 and 192, Apr. 2015.
[10] S. Theodossiades and S. Natsiavas, "Periodic and chaotic dynamics of motor-driven gear-pair systems with backlash," *Chaos Solitons Fractals*, vol. 12, no. 13, pp. 2427–2440, Oct. 2001.
[11] L. Xiang, Y. Zhang, N. Gao, A. J. Hu, and J. T. Xing, "Nonlinear dynamics of a multistage gear transmission system with multi-clearance," *Int. J. Bifurcation Chaos*, vol. 28, no. 3, Mar. 2018, Art. no. 1850034.

[12] J. Y. Yoon and B. Kim, "Effect and feasibility analysis of the smoothening functions for clearance-type nonlinearity in a practical driveline system," *Nonlinear Dyn.*, vol. 85, no. 3, pp. 1651–1664, Aug. 2016.
[13] G. P. Prajapat, P. Bhui, N. Senroy, and I. N. Kar, "Modelling and estimation of gear train backlash present in wind turbine driven DFIG system," *IET Gener. Transm. Distrib.*, vol. 12, no. 14, pp. 3527–3535, Aug. 2018.
[14] F. Yang, G. Liu, H. Yu, Y. Cao, and K. He, "Rigid-flexible coupling dynamic simulation of precision reducer with backlash," in *Proc. 6th Int. Conf. Mech., Automot. Mater. Eng. (CMAME)*, Hong Kong, China, Aug. 2018, pp. 90–94.
[15] Y. Zheng, Z. R. Luo, J. Z. Shang, X. M. Wang, and N. H. Yu, "Dynamics modeling and resonance analysis of anti-backlash gear transmission system based on harmonic balance method," *Adv. Mater. Res.*, vol. 711, pp. 556–561, Jun. 2013.
[16] T. Yang, S. Yan, W. Ma, and Z. Han, "Joint dynamic analysis of space manipulator with planetary gear train transmission," *Robotica*, vol. 34, no. 5, pp. 1042–1058, May 2016.
[17] H. Xu, D. G. Shang, S. Y. Li, and L. X. Gao, "The vibration characteristic research of the transmission system of the rolling mill based on absolute node coordinates," *Appl. Mech. Mater.*, vols. 644–650, pp. 763–768, Sep. 2014.
[18] S. Y. Chen and J. Y. Tang, "Effect of backlash on dynamics of spur gear pair system with friction and time-varying stiffness," *J. Mech. Eng.*, vol. 45, no. 8, pp. 119–124, Aug. 2009.
[19] C. Spitas and V. Spitas, "Coupled multi-DOF dynamic contact analysis model for the simulation of intermittent gear tooth contacts, impacts and rattling considering backlash and variable torque," *Proc. Inst. Mech. Eng., C, J. Mech. Eng. Sci.*, vol. 230, nos. 7–8, pp. 1022–1047, Jul. 2015.
[20] Z. X. Liu, Z. S. Liu, and X. Y. Yu, "Dynamic modeling and response of a spur planetary gear system with journal bearings under gravity effects," *J. Vib. Control*, vol. 24, no. 16, pp. 3569–3586, May 2018.
[21] J.-F. Shi, X.-F. Gou, and L.-Y. Zhu, "Modeling and analysis of a spur gear pair considering multi-state mesh with time-varying parameters and backlash," *Mech. Mach. Theory*, vol. 134, pp. 582–603, Apr. 2019.
[22] A. Fernandez-del-Rincon, P. Garcia, A. Diez-Ibarbia, A. de-Juan, M. Iglesias, and F. Viadero, "Enhanced model of gear transmission dynamics for condition monitoring applications: Effects of torque, friction and bearing clearance," *Mech. Syst. Signal Process.*, vol. 85, no. 1, pp. 445–467, Feb. 2017.
[23] A. Gündüz, Z. B. Saribay, S. Yilmaz, and E. Kaynar, "Mathematical modeling and internal clearance optimization of helicopter high speed bearing systems considering temperature variations," in *Proc. 71st AHS Int. Annu. Forum*, Virginia, BC, USA, Jan. 2015, pp. 2252–2262.
[24] N. Sawalhi and R. B. Randall, "Simulating gear and bearing interactions in the presence of faults: Part I. The combined gear bearing dynamic model and the simulation of localised bearing faults," *Mech. Syst. Signal Process.*, vol. 22, no. 8, pp. 1924–1951, Nov. 2008.
[25] K. Feng, P. Borghesani, W. A. Smith, R. B. Randall, Z. Y. Chin, J. Ren, and Z. Peng, "Vibration-based updating of wear prediction for spur gears," *Wear*, vol. 426, pp. 1410–1415, Apr. 2019.
[26] G. Shen, D. Xiang, K. Zhu, L. Jiang, Y. H. Shen, and Y. L. Li, "Fatigue failure mechanism of planetary gear train for wind turbine gearbox," *Eng. Failure Anal.*, vol. 87, pp. 96–110, May 2018.
[27] H. B. Gao, Y. G. Li, and J. Liu, "Dynamic analysis of a spur gear system with tooth-wear faults based on dynamic backlash," *J. Vib. Shock*, vol. 33, no. 18, pp. 221–226, Sep. 2014.
[28] C. Li and C. L. Cai, "Nonlinear dynamics analysis of a gear-shaft-bearing system with breathing crack and tooth wear faults," *Open Mech. Eng. J.*, vol. 9, no. 1, pp. 483–491, Jul. 2015.
[29] V. Janakiraman, S. Li, and A. Kahraman, "An investigation of the impacts of contact parameters on wear coefficient," *J. Tribol.*, vol. 136, no. 3, pp. 1–7, May 2014.
[30] K. F. Brethee, D. Zhen, F. Gu, and A. D. Ball, "Helical gear wear monitoring: Modelling and experimental validation," *Mech. Mach. Theory*, vol. 117, no. 11, pp. 210–229, Nov. 2017.
[31] R. P. Sekar and R. Sathishkumar, "Enhancement of wear resistance on normal contact ratio spur gear pairs through non-standard gears," *Wear*, vols. 380–381, no. 1, pp. 228–239, Jun. 2017.
[32] S. J. Wu, H. B. Zhang, X. S. Wang, Z. M. Peng, K. K. Yang, and W. L. Zhu, "Influence of the backlash generated by tooth accumulated wear on dynamic behavior of compound planetary gear set," *Proc. Inst. Mech. Eng., C, J. Mech. Eng. Sci.*, vol. 231, no. 11, pp. 2025–2041, Jun. 2017.
[33] A. Kahraman, P. Bajpai, and N. E. Anderson, "Influence of tooth profile deviations on helical gear wear," *J. Mech. Des.*, vol. 127, no. 4, pp. 656–663, Jul. 2005.
[34] R. Kasuba and J. W. Evans, "Extended model for determine dynamic loads in spur gearing," *J. Mech. Des.*, vol. 103, no. 2, pp. 398–409, Apr. 1981.

YING-KUI GU was born in Nanyang, Henan, China, in 1976. He received the B.S. and M.S. degrees from the Jiangxi University of Science and Technology, Ganzhou, Jiangxi, China, in 1998 and 2002, respectively, and the Ph.D. degree from the Dalian University of Technology, Dalian, China, in 2005, all in mechanical engineering.

From 2005 to 2009, he was an Assistant Professor with the School of Mechanical and Electronical Engineering, Jiangxi University of Science and Technology, where he has been a Professor, since 2009. He has held visiting appointments at the University of Albert, Canada, in 2011. He is the author of three books and more than 60 journal papers. His research interests include reliability engineering, fault diagnosis, and optimization design.

Dr. Gu is also a (Senior) Member of several professional societies and has served on the boards of professional societies. He was selected to the New Century National Hundred, Thousand and Ten Thousand Talent Project in Jiangxi Province, in 2007, and to the Young Scientists Object Program of Jiangxi Province, in 2014.

WEN-FEI LI received the B.S. degree in mechanical engineering from the Jiangxi University of Science and Technology, China, in 2017, where he is currently pursuing the master's degree in mechanical engineering. His research interests include reliability engineering and fault diagnosis.

JUN ZHANG received the B.S. degree in mechanical engineering from the Henan University of Technology, in 2015. He is currently pursuing the master's degree in mechanical engineering with the Jiangxi University of Science and Technology. His research interests include reliability engineering and fault diagnosis.

GUANG-QI QIU received the B.S. degree from Yanshan University, Qihuangdao, China, in 2009, the M.S. degree from the Jiangxi University of Science and Technology, Ganzhou, Jiangxi, China, in 2014, and the Ph.D. degree from the Huanan University of Science and Technology, Guangzhou, China, in 2017, all in mechanical engineering. He is currently an Assistant Professor with the School of Mechanical and Electronical Engineering, Jiangxi University of Science and Technology. He has published ten journal papers in the fields of reliability engineering, optimization design, and product development. His current research interests include reliability engineering and fault diagnosis.